Annals of Microbiology (2019) 69:1247–1257
https://doi.org/10.1007/s13213-019-01508-0

ORIGINAL ARTICLE

Analysis of the influence of cyclo (L-phenylalanine-L-proline) on the proteome of *Staphylococcus aureus* using iTRAQ

Duiyuan Ai[1,2] · Weibing Zhang[1] · Jianmin Yun[1] · Yingying Cao[1]

Received: 11 April 2019 / Accepted: 2 August 2019 / Published online: 14 August 2019

Abstract

Purpose Cyclo (L-phenylalanine-L-proline) (cFP) is an extracellular quorum sensing (QS) signal molecule that coordinates communication between Gram-negative bacteria. Some studies have also reported QS in Gram-positive bacteria. However, the effect of cFP on Gram-positive bacteria remains unknown. Therefore, an isobaric tags for relative and absolute quantitation (iTRAQ) proteomic experiment were designed to elucidate whether cFP influences protein expression in *Staphylococcus aureus* (*S. aureus*).

Methods The iTRAQ proteomics method was used to analyze untreated (control) and *S. aureus* treated with cFP for 12 h. Samples were then processed by liquid-phase tandem mass spectrometry (LC-MS/MS) and analyzed using bioinformatics tools.

Results The results identified 1296 proteins from the *S. aureus* CGMCC 1.1861 proteome. Twenty-two proteins, including some two-component regulatory systems (TCRS), were associated with signal transduction. Differential expression analysis revealed that only 43 proteins were up-regulated and 41 proteins were down-regulated by cFP. The most significantly different pathways were amino acid metabolism, fatty acid degradation, and metabolism of cofactors and vitamins. Results showed that cFP down-regulated virulence factors, up-regulated lipid and amino acid metabolism, promoted acetylation and phosphorylation, and decreased alcohol dehydrogenase expression. A total of 12 significantly differentially expressed proteins (DEPs) were related to signal transduction. Among them, Rot (Q9RFJ6) and SarR (Q9F0R1), which can inhibit transcription of the Agr system, were up-regulated, whereas virulence factors such as ESAT-6 protein A (Q2G189), phenol soluble modulin (Psm, Q2FZA4), and a peptide ABC transporter permease (Q2G168) were down-regulated. AgrA (Q2FWM4) was down-regulated by cFP in *S. aureus*.

Conclusion cFP reduced AgrA and the expression of some exotoxins but increased Rot and SarR expression.

Keywords Cyclic dipeptide · Quorum sensing · Two-component regulatory systems · Signal pathway · Pathogenicity

Introduction

Quorum sensing (QS) is a very important mechanism for coordinating the social behavior of bacteria to adapt to different environments according to their population densities (Banerjee and Arun 2017). QS involves the production of and response to extracellular signaling molecules called autoinducers (AIs) (Kumari et al. 2006). Some common QS phenotypes include group behaviors such as competence, colonization, motility, biofilm formation, virulence factor expression, and stress responses (Kavanaugh and Horswill 2016; Eickhoff and Bassler 2018; Bettenworth et al. 2019; Jiang et al. 2019; Zhao et al. 2019). Certain bacteria are also able to use QS to regulate bioluminescence, nitrogen fixation, and sporulation (Kavanaugh and Horswill 2016; Rutherford and Bassler 2012). Some genes are modified in response to a threshold AI concentration that depends on high cell density. This mechanism can alter local surface tension enough to create Marangoni flows, which facilitate swarming and colony motility (Daniels et al. 2006). In Gram-negative bacteria, typical QS molecules are N-acyl homoserine lactones (AHL) or other molecules whose production depends on S-adenosylmethionine as a substrate (Wei et al. 2011). In

Electronic supplementary material The online version of this article (https://doi.org/10.1007/s13213-019-01508-0) contains supplementary material, which is available to authorized users.

✉ Duiyuan Ai
156797555@qq.com; aidy@gsau.edu.cn

[1] College of Food Science and Engineering, Gansu Agricultural University, Lanzhou, Gansu, People's Republic of China

[2] Food Science and Engineering, Gansu Agricultural University, No. 1, Yingmen Village, Fuqiang Road, Anning Area, Lanzhou city, Gansu Province, China

general, AHLs can bind directly to transcription factors (TFs) to up-regulate or down-regulate relative gene expression (Bassler 1999). Gram-positive bacteria typically use two-component regulatory systems (TCRS) with autoinducing peptides (AIP) such as oligopeptides for QS (Rutherford and Bassler 2012). AIP binds to a membrane-bound histidine kinase receptor (HK) to auto-phosphorylate and activate their cognate cytoplasmic response regulator. The phosphorylated response regulator activates transcription of genes in the QS regulon. Another possible mechanism is direct AIP binding to a TF that initiates or inhibits transcription (Rutherford and Bassler 2012).

In Gram-positive QS circuits, the pro-AIP, transporter, HK, and TF are typically encoded in an operon (Ji et al. 1995; Peterson et al. 2000). Expression of this operon is activated by the phosphorylated response regulator, initiating an auto-inducing feed-forward loop that synchronizes the QS response. The *Staphylococcus aureus* accessory gene regulator (Agr) system is a model Gram-positive QS system also known as a TCRS signal transduction pathway (Thoendel et al. 2011). When the concentration of the signal molecule reaches a threshold, the membrane-bound HK AgrC is phosphorylated, stimulating the Agr system. The AIP precursor is synthesized via AgrD, processed into the mature AIP octapeptide, and transported out of the cell by AgrB. The AIP is then detected by AgrC and the TF AgrA is phosphorylated by phosphorylated AgrC. AgrA can then activate the *agr* P2 (RNAII) and P3 (RNAIII) promoters. RNAIII post-transcriptionally activates expression of virulence factors and represses Rot, which is the main repressor of toxin genes encoding virulence factors. Gram-positive bacteria can initiate pathogenic processes via QS circuits that allow for detection of cell population density. The final consequence of this QS regulatory cascade is down-regulation of surface virulence factors such as protein A (*spa*) and up-regulation of secreted virulence factors such as α-toxin and σ-toxin (Rutherford and Bassler 2012; Kavanaugh and Horswill 2016). In *S. aureus*, some researchers have suggested that the Agr system inhibits biofilm formation (Vuong et al. 2000; Boles and Horswill 2008). This leads bacteria to establish biofilm communities at low cell densities but terminate biofilm production and decrease surface proteins and adhesions once they reach high cell densities. In this way, the cell is able to secrete virulence factors that facilitate its dispersal and invasion (Yarwood et al. 2004; Boles and Horswill 2008).

Cyclo (L-phenylalanine-L-proline) (cFP) is a cyclic dipeptide formed by the condensation of two amino acids also called 2, 5-diketopiperazines. It consists of a stable, six-membered ring structure, which includes one hydrogen donor and four acceptor bonds (Hu et al. 2019). This makes it an active ligand with key roles in protein binding. It is a secondary metabolite produced by numerous fungi as well as Gram-positive and Gram-negative bacteria (Prasad 1995; Huang et al. 2010; Brack et al. 2014; Mishra et al. 2017). In Gram-negative bacteria such as *Pseudomonas* spp., cFP was shown to be part of a novel class of AIs that uses *lux*-based AHL biosensors (Bellezza et al. 2014). Furthermore, cFP can reduce bioluminescence and biofilm formation (Kim et al. 2013), induce the virulence factor OmpU to influence host–pathogen interactions in *Vibrio vulnificus* (Park et al. 2006), up-regulate pathogenicity and toxin proteins such as Ctx in *Vibrio cholera* (Bina et al. 2013), decrease toxic shock syndrome toxin-1 (TSST-1) expression (Li et al. 2011), and inhibit serine/threonine protein kinase (Akt) (Hong et al. 2008). cFP is a very small molecule that can be easily obtained by fermentation or synthesis (Park et al. 2006). Its multiple uses include clinical applications as an antibiotic prophylaxis and inhibition of biofilm formation and multi-drug resistance in bacteria (Rhee 2004; Pan and Ren 2009; Kim et al. 2015). Recently, it was found to be toxic to tumor cells and can inhibit virus and human innate immunity (Brauns et al. 2004; Brauns et al. 2005; Chen et al. 2018; Kwak et al. 2018; Lee et al. 2018). However, the study of cFP has focused mainly on LuxR-mediated QS systems in bacteria, while its signal transduction mechanism, binding receptors, and in particular its effect on Gram-positive bacteria remain unknown. One transcriptomic study of *V. vulnificus* indicated that cFP up-regulated transport and metabolism of inorganic molecules and down-regulated glycolysis, anaerobic energy metabolism, and the pyruvate oxidase system (Kim et al. 2013). It was also found that cFP acts as a quorum quenching agent to inhibit Agr (Li et al. 2011; Tang and Zhang 2014).

Isobaric tags for relative and absolute quantitation (iTRAQ) are a proteome quantification technique that can be used to analyze up to eight samples in one experiment (Wiese et al. 2007) and can be used for high-throughput generation of abundant, repeatable, high-resolution data with high quantitative accuracy (Chai and Zhao 2017). This technology, developed by Applied Biosystems Inc., has been widely used since it was first proposed by Ross et al. (2004) at a mass spectrometry (MS) conference. In 2009, more than 150 research articles reported using this method, and it is now the most common procedure for proteomic analysis. iTRAQ labeling coupled with multidimensional liquid chromatography and MS analysis (LC-MS/MS) is a gel-free quantitative proteomics technology that uses amine-specific isobaric tags to compare the intensity of reporter ions of labeled peptides and infer quantitative values for corresponding proteins (DeSouza et al. 2005; Zhang et al. 2017). In this study, iTRAQ was conducted to elucidate the influence of cFP on protein expression in *S. aureus*. This work provides crucial clues about how cFP affects the QS mechanism via TCRS, especially the main QS system AgrC/A, through analysis of differential protein expression.

Materials and methodsBacteria and reagents

Staphylococcus aureus subsp. aureus CGMCC1.1861 (ATCC 6538P; *S. aureus* 1.1861), supplied by the China General Microbiological Culture Collection Center (CGMCC, Beijing, China), is a positive control strain used in medicine and microbial hygiene tests (Holowachuk et al. 2003; Holowachuk et al. 2004). cFP (IUPAC name: (3S,8aS)-3-benzyl-2,3,6,7,8,8a-hexahydropyrrolo[1,2-a]pyrazine-1,4-dione, CAS number: 3705-26-8) was synthesized by Nanjing Peptide Biotech Ltd. (Nanjing, China). *S. aureus* 1.1861 was previously shown to be sensitive to cFP in growth curves (Duiyuan 2017). It was grown in basic nutrient beef extract peptone media in Erlenmeyer flasks at 37 °C with shaking for 18 h. After continuous culture for two generations, cells were diluted to an optical density at 600 nm (OD_{600}) of 0.1 per mL and 100 mL was separated into one Erlenmeyer flask for each condition. The prepared samples were divided into two groups. Control (CK) samples of *S. aureus* treated with 0.1 mL dimethylsulfoxide (DMSO) were cultured at 37 °C with shaking for 12 h in basic nutrient beef extract peptone media. Treatment group (cFP) samples of *S. aureus* treated with cFP dissolved in 0.1 mL DMSO at a final concentration of 10 mM were cultured for 12 h in the same conditions. Each group included three independent replicates (i.e., CK-1, CK-2, and CK-3 in the control group and cFP-1, cFP-2, and cFP-3 in the treatment group). Both groups were collected by centrifugation at 1200×*g* for 5 min at 4 °C and frozen in liquid nitrogen until further analysis.

iTRAQ proteomic experimentThe iTRAQ workflow is illustrated in Fig. 1. Total protein was extracted from processed samples using the cold acetone method (Xiao et al. 2017). Samples were ground to a powder in liquid nitrogen, dissolved in 2-mL lysis buffer (8 M urea, 2% SDS, and 1× protease inhibitor cocktail (Roche Ltd., Basel, Switzerland)), sonicated on ice for 30 min, and centrifuged at 13,000 rpm for 30 min at 4 °C. The supernatant was transferred to a fresh tube. For each sample, proteins were precipitated with ice-cold acetone at − 20 °C overnight. The precipitates were washed with acetone three times and re-dissolved in 8 M urea with sonication on ice. Protein quality was examined by SDS-PAGE.

A Bradford protein concentration assay (BCA) kit (P0010S, Beyotime Institute of Biotechnology, Beijing, China) was used to determine the protein concentration of the supernatant. A total of 100 μg protein was transferred to a new tube and adjusted to a final volume of 100 μL with 8 M urea. A total of 11 μL of 1 M DL-dithiothreitol was added and samples were incubated at 37 °C for 1 h. Then, 120 μL of 55 mM iodoacetamide was added and the sample was incubated for 20 min at room temperature and protected from light. For each sample, proteins were precipitated with ice-cold acetone and re-dissolved in 100-μL triethylammonium bicarbonate buffer. Proteins were then tryptic digested with sequence-grade modified trypsin (Promega, Madison, WI, USA) at 37 °C overnight. The resulting peptide mixture was covalently labeled with stable isotope molecules with the following tags introduced from iTRAQ-specific reagents to the N-terminus and side chain amines of peptides according to the manufacturer's instructions: control group CK-1 with a 113 mass isotope tag; CK-2 with a 114 tag; CK-3 with a 115 tag; and treatment group cFP-1 with a 116 tag; cFP-2 with a 117 tag; and cFP-3 with a 118 tag. The labeled samples were combined and dried in a vacuum (Zhang et al. 2017).

Labeled samples were combined and subjected to strong cation exchange fractionation on a column connected to a high-performance liquid chromatography system. The peptide mixture was dissolved in buffer A (20 mM ammonium formate in water, pH adjusted to 10.0 with ammonium hydroxide) and fractionated by high pH separation using an Ultimate 3000 system (Thermo Fisher Scientific, Waltham, MA, USA) connected to a reverse-phase column. Peptide fractions were resuspended in 30-μL solvent C (0.1% formic acid in water) or D (0.1% formic acid in acetonitrile), separated by nanoLC, and analyzed by on-line electrospray tandem mass spectrometry. Experiments were performed on an Easy-nLC 1000 system (Thermo Fisher Scientific) connected to an Orbitrap Fusion Tribrid mass spectrometer (Thermo Fisher Scientific) equipped with an online nano-electrospray ion source. Survey full-scan mass spectra (m/z 350–1550) were acquired with a mass resolution of 120 K, followed by sequential high energy collisional dissociation tandem mass spectrometry scans with a resolution of 30 K. The isolation window was set to 1.6 Da. The AGC target was set to 400,000. The fixed first mass was

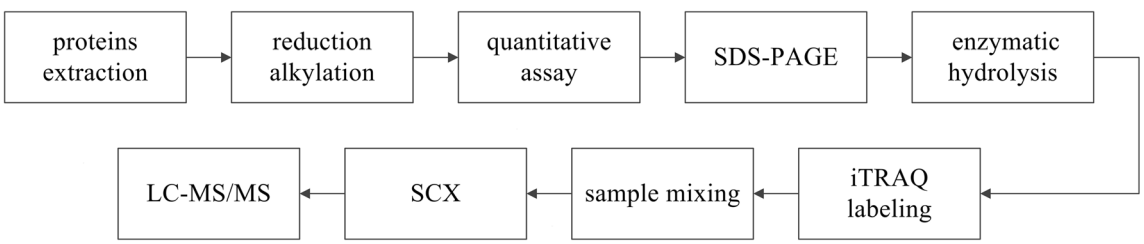

Fig. 1 iTRAQ workflow. Abbreviations: SDS-PAGE, sodium dodecyl sulfate polyacrylamide gel electrophoresis; LC-MS/MS, liquid phase tandem mass spectrometry analysis; SCX, strong cation exchange chromatography separation

set to 110. In all cases, one microscan was recorded using a dynamic exclusion of 45 s (Chai and Zhao 2017).

Database analysisMass spectrometry data were transformed into Mascot generic format (MGF) files using Proteome Discovery 1.2 (Thermo, Pittsburgh, PA, USA) and analyzed using the Mascot search engine version 2.3.2 (Matrix Science, London, UK) (Fig. 2). The Mascot database was set up for protein identification using the reference transcriptome or NCBInr/SwissProt/Uniprot/IPI database. Mascot was searched with a fragment ion mass tolerance of 0.050 Da and a parent ion tolerance of 10.0 ppm. NCTC 8325 is the only reference proteome in Uniprot (UP000008816, strain NCTC 8325, protein count: 2889, https://www.uniprot.org/proteomes/UP000008816) and is well studied and annotated (Gillaspy et al. 2006). Therefore, it was selected as the main reference proteome for our data search results. The Kyoto Encyclopedia of Genes and Genomes (KEGG) (Kanehisa et al. 2008) pathway enrichment analysis was used to identify differentially expressed proteins (DEPs) significantly enriched in metabolic or signal transduction pathways when compared with the entire proteome. The following formula was used to calculate P values:

$$P = 1 - \sum_{i=0}^{m-1} \frac{\binom{M}{i}\binom{N-M}{n-i}}{\binom{N}{n}}$$

where N is the number of all genes with a KEGG annotation, n is the number of DEPs in N, M is the number of genes annotated to specific pathways, and m is the number of DEPs in M. The calculated P values were adjusted using the false discovery rate (FDR) correction with FDR ≤ 0.05 set as the threshold. Pathways meeting this condition were defined as pathways significantly enriched in DEPs.

ResultsProtein identification and quantificationProteomics experiments referring to the NCBInr/SwissProt/Uniprot/IPI database identified 1296 *S. aureus* proteins in both control and treatment groups (Table S1). Mascot search results were averaged using medians and quantified. Proteins with a fold change > 1.2 or < 0.83 and an unadjusted significance level of $P < 0.05$ were considered differentially expressed. In total, 1153 proteins were quantitative statistics and annotated by KEGG (Table S2). Of these, 43 proteins were significantly up-regulated and 41 proteins were down-regulated in cFP treatment groups compared with controls ($P < 0.05$; Table 1, Table S3). These results revealed clues about target proteins influenced by cFP. The adenosylmethionine-8-amino-7-oxononanoate aminotransferase protein BioA (Q2FVJ6) was the most up-regulated protein, followed by the biotin synthase protein BioB and four ribonuclease M5 proteins. A total of 12 proteins were directly related to transcription and signal transduction among these 84 DEPs, including the up-regulated proteins Rot (Q9RFJ6), acetyl-CoA acetyltransferase (Q2G0K2), SarR (Q9F0R1), MalR (A0A0Y9ARI8), MalR (Q2FY63), transcription factor (TF) (Q2FWG9), and PhoP (Q2FXN6) and the down-regulated proteins ATP-binding Cassette (ABC, Q2G168), RpiR TF (Q2FVV2), EsxA (Q2G189), TF (Q2G2H0), and phenol soluble modulin beta 1 (Psm, Q2FZA4) (Table 2).

Pathway annotation and enrichmentIn this study, 522 proteins from the treated and control groups were found to be associated with known pathways (Table S4). The most enriched pathway was carbon metabolism, which included 77 proteins, followed by biosynthesis of amino acids with 61 proteins, ribosome with 54 proteins, purine with 38 proteins, pyruvate with 37 proteins, pyrimidine with 34 proteins, and glycolysis/gluconeogenesis with 33 proteins. In addition, 22 proteins were related to signal transduction (Table S4, Fig. S7). Nineteen ABC transporters and 11 proteins related to *S. aureus* infection were identified.

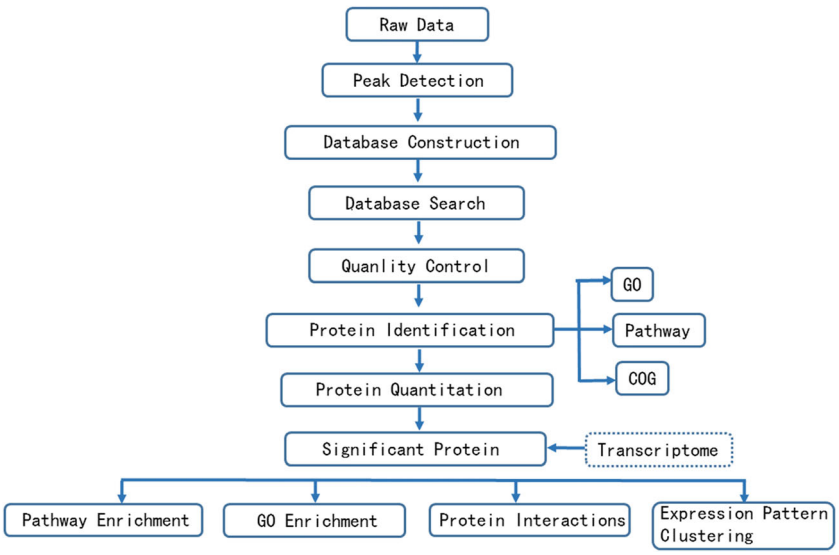

Fig. 2 Proteomic analysis workflow. The raw data were transformed and analyzed using Mascot software. These data were then assessed for protein identification using the NCBInr/SwissProt/Uniprot/IPI database. Afterwards, identified proteins were quantified to identify significantly differentially expressed proteins (DEPs). Finally, DEPs were analyzed for KEGG pathway enrichment, Gene Ontology (GO) enrichment, and protein interactions to identify mechanisms at the overall proteome level

Table 1 Significantly differentially expressed proteins between control and cFP-treated *S. aureus*

Gene ID	Control	cFP	log2_FC (cFP/CK)	*P* value	FDR	Description
Q2FVJ6	0.9643	2.5560	1.4063	0.0003	0.0579	adenosylmethionine--8-amino-7-oxononanoate aminotransferase BioA
Q2FVJ7	0.8913	1.8340	1.0410	0.0005	0.0701	biotin synthase BioB
A0A0H2I6U0	1.0313	1.9283	0.9028	0.0256	0.2943	ribonuclease M5
G5JJ45	1.0313	1.9283	0.9028	0.0256	0.2943	ribonuclease M5
A0A1E5JK13	1.0313	1.9283	0.9028	0.0256	0.2943	ribonuclease M5
Q2G0T1	1.0313	1.9283	0.9028	0.0256	0.2943	ribonuclease M5
Q9RFJ6	0.9387	1.6023	0.7715	0.0001	0.0420	HTH-type transcription factor (TF) Rot
Q2G0K2	0.9647	1.3957	0.5329	0.0013	0.1087	acetyl-CoA acetyltransferase
Q2FZW2	1.2047	1.7410	0.5313	0.0458	0.3567	NifU-like protein, Nitrogen fixation protein NifU
Q2FY46	0.8717	1.2583	0.5297	0.0348	0.3185	exodeoxyribonuclease 7 large subunit
Q2FZU3	1.0110	1.3960	0.4655	0.0038	0.1835	glycerophosphodiester phosphodiesterase
Q2G1P3	1.1097	1.5273	0.4609	0.0439	0.3501	oleate hydratase
Q2G0V3	0.8693	1.1930	0.4566	0.0118	0.2372	cystathionine beta-lyase
Q2G1U0	0.9663	1.3233	0.4536	0.0090	0.2372	chain a, molecular mechanism and evolution of guanylate kinase regulation by (p)ppgpp
Q2G002	1.0747	1.4667	0.4487	0.0478	0.3627	3-dehydroquinase
Q9F0R1	1.1597	1.5650	0.4325	0.0176	0.2821	HTH-type TF SarR
Q2G024	1.1650	1.5607	0.4218	0.0418	0.3463	ribonuclease R
Q2G228	0.9853	1.3023	0.4024	0.0430	0.3495	purine nucleoside phosphorylase
A0A0Y9ARI8	1.1453	1.5100	0.3988	0.0323	0.3133	Maltose operon transcriptional repressor MalR, LacI family
Q2FY63	1.1453	1.5100	0.3988	0.0323	0.3133	LacI family TF
Q2FXI5	1.0217	1.3190	0.3685	0.0208	0.2879	peptidase M28
Q2G0R1	0.9127	1.1760	0.3657	0.0199	0.2836	hypoxanthine phosphoribosyl transferase
Q2FY16	1.1943	1.5247	0.3523	0.0440	0.3501	deoxyribonuclease IV
Q2G1D0	0.9067	1.1473	0.3396	0.0101	0.2372	acetyl-CoA acetyltransferase
Q2FWG9	1.0047	1.2707	0.3389	0.0474	0.3621	CsoR family TF
Q2FWY9	1.0640	1.3377	0.3302	0.0041	0.1835	glutamyl-tRNA(Gln) amidotransferase
Q2FYZ0	1.0453	1.3063	0.3216	0.0045	0.1835	glutathione peroxidase
Q2FX00	1.0497	1.3063	0.3156	0.0221	0.2879	glutamine amidotransferase
Q2FXG1	1.0327	1.2837	0.3139	0.0329	0.3133	GTP cyclohydrolase II
A0A1E5JEN8	1.0327	1.2837	0.3139	0.0329	0.3133	3,4-dihydroxy-2-butanone-4-phosphate synthase
Q2FWB8	1.0053	1.2487	0.3127	0.0015	0.1138	purine nucleoside phosphorylase, partial
Q2FXN6	0.9707	1.2030	0.3096	0.0056	0.1870	DNA-binding response TF
Q2FVW7	1.0340	1.2800	0.3079	0.0151	0.2698	acyl-CoA dehydrogenase, N-terminal domain protein
Q2G101	0.9607	1.1887	0.3072	0.0010	0.0897	Phosphoglycerate mutase family protein
Q2FY51	1.0273	1.2697	0.3055	0.0315	0.3133	dihydrolipoyl dehydrogenase
Q2FWG2	0.9450	1.1630	0.2995	0.0300	0.3112	hydroxyethylthiazole kinase
Q2G202	0.9307	1.1403	0.2931	0.0399	0.3423	Hemoglobin-like protein HbO
Q2G0V7	0.9817	1.1963	0.2853	0.0116	0.2372	carboxylesterase
Q2G0Z5	1.0040	1.2163	0.2768	0.0371	0.3336	NADPH-dependent oxidoreductase
A0A077UYP2	0.9973	1.2070	0.2753	0.0050	0.1856	Free methionine-(R)-sulfoxide reductase
Q2FZY5	1.1173	1.3457	0.2683	0.0305	0.3133	cysteine desulfurase
Q2G241	0.9477	1.1390	0.2653	0.0060	0.1920	glutamate--tRNA ligase
Q2FVT6	1.0117	1.2153	0.2646	0.0197	0.2834	imidazolonepropionase
Q2FW23	0.9600	0.7923	− 0.2769	0.0171	0.2811	30S ribosomal protein S5
Q2FUX7	1.0367	0.8457	− 0.2938	0.0326	0.3133	arginine deiminase ArcA
Q2G2E9	0.9540	0.7770	− 0.2961	0.0215	0.2879	TIGR04141 family sporadically distributed protein
Q2FVG3	0.9147	0.7440	− 0.2979	0.0292	0.3102	carboxylesterase

Table 1 (continued)

Gene ID	Control	cFP	log2_FC (cFP/CK)	*P* value	FDR	Description
Q2FXH8	0.9857	0.7977	− 0.3053	0.0001	0.0318	Uncharacterised protein
Q2G261	1.0030	0.8057	− 0.3161	0.0256	0.2943	superoxide dismutase
Q2FZA1	0.9723	0.7793	− 0.3192	0.0195	0.2834	GNAT family N-acetyltransferase
Q2G0S5	1.0157	0.8090	− 0.3282	0.0001	0.0318	stage V sporulation protein G
Q2FXP2	1.0137	0.8057	− 0.3313	0.0088	0.2372	Glyceraldehyde 3-phosphate dehydrogenase
Q2FZP9	0.9203	0.7267	− 0.3409	0.0447	0.3529	2′-5′ RNA ligase
P0A0G2	1.0553	0.8320	− 0.3430	0.0424	0.3468	50S ribosomal protein L30, partial
Q2FVT2	1.0050	0.7917	− 0.3442	0.0016	0.1153	formimidoylglutamase
Q2FVN2	1.1210	0.8780	− 0.3525	0.0481	0.3627	Hsp20/alpha crystallin family protein
Q2FVE0	1.0553	0.8263	− 0.3529	0.0008	0.0857	Alkyl hydroperoxide reductase AhpD
A0A0H3JWD7	0.9387	0.7340	− 0.3548	0.0339	0.3179	pathogenicity island protein
Q2FWB1	0.9870	0.7653	− 0.3670	0.0001	0.0318	oxidoreductase
A0A0H3JPH0	0.9910	0.7683	− 0.3672	0.0469	0.3601	UDP-N-acetylglucosamine 4,6-dehydratase
Q2G1K7	0.8443	0.6463	− 0.3855	0.0463	0.3583	capsular polysaccharide synthesis enzyme CapB
Q2G168	0.8967	0.6863	− 0.3857	0.0195	0.2834	peptide ABC transporter permease
Q7X2S2	1.0727	0.8140	− 0.3981	0.0046	0.1835	carbamate kinase 2 ArcC2
A0A1E5JBN2	1.0297	0.7493	− 0.4585	0.0412	0.3457	SH3-like domain protein
Q2FYS7	1.0113	0.7357	− 0.4591	0.0004	0.0639	iron-sulfur cluster biosynthesis family protein
Q2FYH7	0.9120	0.6453	− 0.4990	0.0128	0.2423	chromosome replication protein DnaD
A0A0U1MPU9	0.9673	0.6643	− 0.5421	0.0164	0.2793	Putative staphylococcal protein
Q2FV95	1.1630	0.7903	− 0.5573	0.0348	0.3185	L-serine dehydratase, iron-sulfur-dependent subunit alpha
Q2G1I8	1.1310	0.7617	− 0.5704	0.0057	0.1870	Uncharacterised protein
A0A1Q8DFZ6	1.0253	0.6903	− 0.5707	0.0245	0.2943	Uncharacterised protein
Q2G2J7	1.0233	0.6773	− 0.5953	0.0123	0.2372	Uncharacterised protein
A0A133QBW6	1.0233	0.6773	− 0.5953	0.0123	0.2372	Uncharacterised protein
Q2FVV2	1.0243	0.6513	− 0.6532	0.0028	0.1539	MurR/RpiR family TF
A0A1E5JI47	1.0243	0.6513	− 0.6532	0.0028	0.1539	helix-turn-helix domain, rpiR family protein
A0A0H3JNW6	0.9730	0.6153	− 0.6611	0.0116	0.2372	Uncharacterised protein
Q2G189	1.1733	0.7290	− 0.6866	0.0276	0.3068	virulence factor EsxA
Q2FV94	1.2410	0.6990	− 0.8281	0.0120	0.2372	L-serine dehydratase, iron-sulfur-dependent subunit beta
Q2G1K9	1.1357	0.6363	− 0.8357	0.0027	0.1539	bifunctional acetaldehyde-CoA/alcohol dehydrogenase
P0C818	1.0510	0.5730	− 0.8752	0.0152	0.2698	PsmA4, Phenol-soluble modulin alpha 4 peptide
A0A0Z0SZ51	0.9583	0.4723	− 1.0207	0.0186	0.2821	Lipase
Q2FYU5	1.0350	0.4783	− 1.1135	0.0085	0.2372	30S ribosomal protein S14
Q2FZA4	1.3880	0.6073	− 1.1924	0.0106	0.2372	phenol soluble modulin Psm
Q2G2H0	1.1243	0.4717	− 1.2532	0.0106	0.2372	TF
Q2G2F5	0.9063	0.3073	− 1.5602	0.0348	0.3185	UDP-GlcNAc 2-epimerase

Furthermore, we identified, compared, and predicted the possible functions of identified proteins and determined their functional classification using the Clusters of Orthologous Groups of proteins (COG) database (Fig. 3). In total, 1038 proteins were annotated (Table S5) and categorized into 20 groups (C-V). Abundant clusters included J: translation, ribosomal structure, and biogenesis with 123 proteins; C: energy production and conversion with 87 proteins; E: amino acid transport and metabolism with 87 proteins; K: transcription with 86 proteins; and carbohydrate transport and metabolism with 78 proteins. A total of 29 proteins were associated with signal transduction mechanisms.

Pathway enrichment analysis was based on KEGG pathways and we applied a hypergeometric test to find pathways that were significantly enriched in DEPs between control and treatment groups compared to all identified background proteins. Significantly enriched pathways were used to determine the most important biochemical, metabolic, and signal transduction pathways associated with DEPs (Fig. 4, Fig. S8, Table S6). As shown in Fig. 4, based on Q-values, the

Table 2 Significantly differentially expressed signal transduction proteins between control and cFP-treated *S. aureus*

Gene ID	Control	cFP	log2_FC (cFP/CK)	*P* value	FDR	Description
Q9RFJ6	0.9387	1.6023	0.7715	0.0001	0.0419	Rot, HTH-type transcription factor (TF)
Q2G0K2	0.9647	1.3957	0.5329	0.0013	0.1087	acetyl-CoA acetyltransferase, Environmental Information
Q9F0R1	1.1597	1.5650	0.4325	0.0176	0.2821	SarR, HTH-type TF,
A0A0Y9ARI8	1.1453	1.5100	0.3988	0.0323	0.3133	MalR, HTH-type Maltose operon TF repressor, LacI family
Q2FY63	1.1453	1.5100	0.3988	0.0323	0.3133	MalR, Maltose operon transcriptional TF, LacI family
Q2FWG9	1.0047	1.2707	0.3389	0.0474	0.3621	TF, cytosolic protein, CsoR family
Q2FXN6	0.9707	1.2030	0.3096	0.0056	0.1870	PhoP, DNA-binding response, phosphate limitation-assimilation, OmpR family
Q2G168	0.8967	0.6863	− 0.3857	0.0195	0.2834	peptide ABC transporter permease
Q2FVV2	1.0243	0.6513	− 0.6532	0.0028	0.1538	TF, carbohydrate derivative metabolic process, MurR/RpiR family
Q2G189	1.1733	0.7290	− 0.6866	0.0276	0.3067	EsxA, virulence factor extracellular protein A
Q2G2H0	1.1243	0.4717	− 1.2532	0.0106	0.2371	TF, DUF1811 domain-containing protein
Q2FZA4	1.388	0.6073	− 1.1924	0.0106	0.2371	Psm, phenol soluble modulin beta 1, Pathogenesis

significantly enriched KEGG class B pathways were amino acid metabolism, lipid metabolism, and metabolism of cofactors and vitamins. Glycine, serine, and threonine metabolism ($P = 0.0108$); riboflavin metabolism ($P = 0.0155$); fatty acid degradation ($P = 0.0299$); and valine, leucine, and isoleucine degradation ($P = 0.0496$) were classified as class C pathways.

DiscussionAnalysis of cFP-treated and control groups revealed that up-regulated proteins included two TCRS receptors, Rot (Q9RFJ6) and SarR (Q9F0R1), and an acetyl-CoA

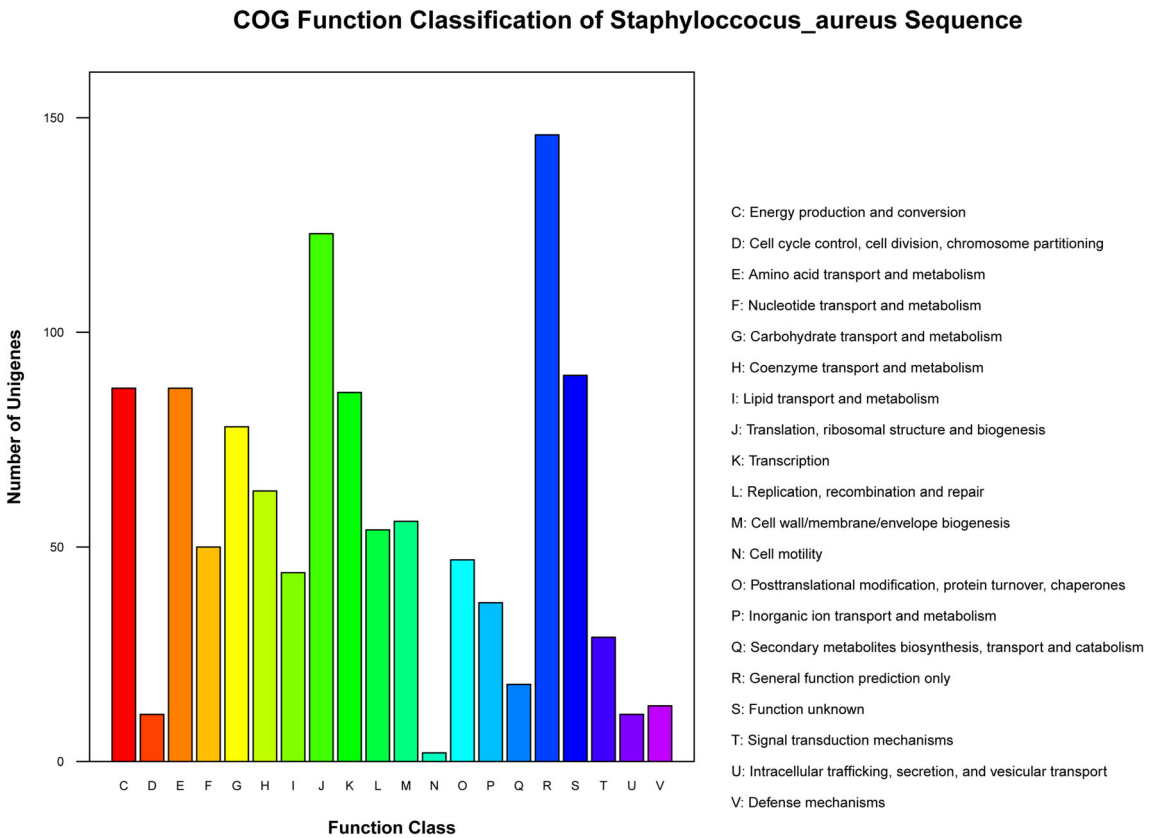

Fig. 3 Clusters of orthologous groups (COG) of protein-based classification of *S. aureus* proteins. Using the COG database, 1038 proteins were classified into 20 groups (C-V). Abundant clusters included R: general function with 146 proteins; J: translation with 123 proteins; S: function unknown with 90 proteins; C: energy production and conversion with 87 proteins; and E: amino acid transport and metabolism with 87 proteins

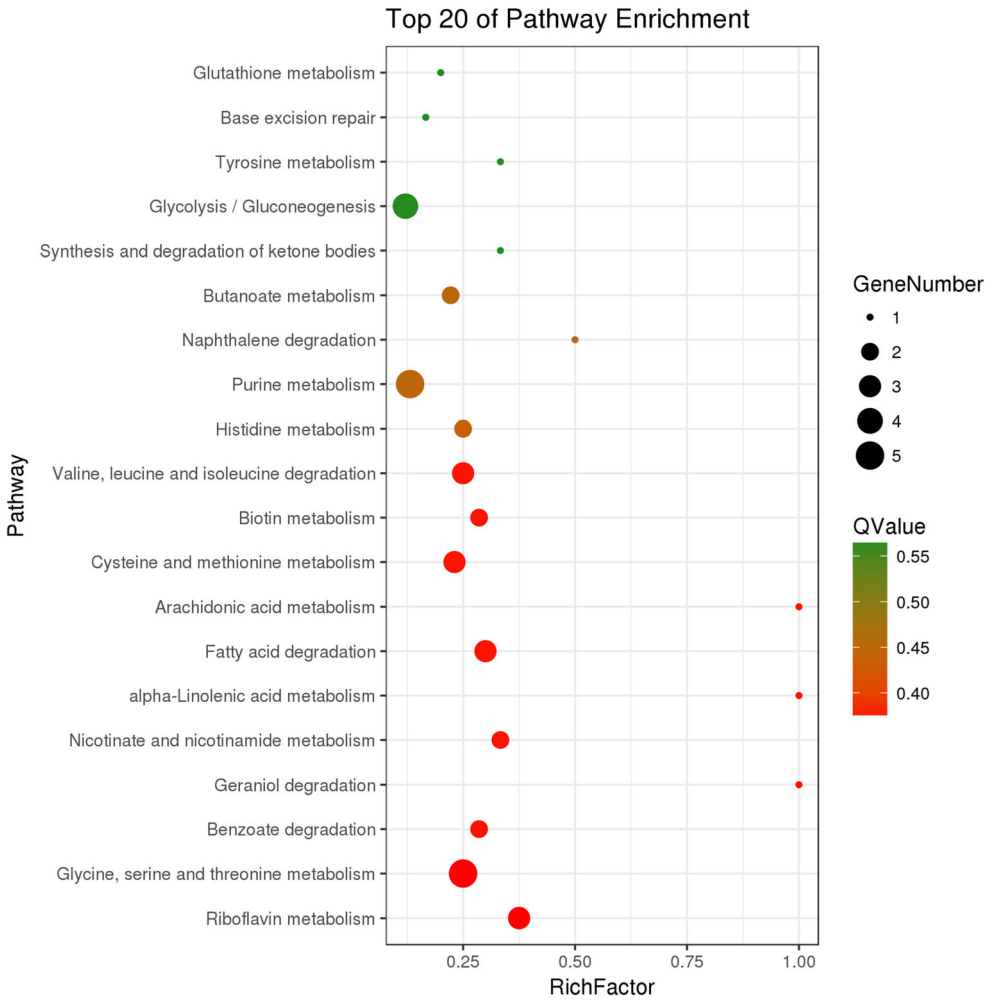

Fig. 4 Top 20 enriched pathways of *S. aureus* proteins influenced by cFP. The *Y*-axis represents pathways and the *X*-axis represents their corresponding RichFactor. A larger area indicates a greater number of DEPs, and the color (from white to red; QValue) indicates the greatest difference in protein expression between the control and treatment groups. The most significantly differentially expressed pathways were glycine, serine, and threonine metabolism ($P = 0.0108$), riboflavin metabolism ($P = 0.0155$), fatty acid degradation ($P = 0.0299$), and valine, leucine, and isoleucine degradation ($P = 0.0496$)

acetyltransferase (Q2G0K2). In addition, some DNA-binding TFs such as MalR (Q2FY63), SAOUHSC_02322 (Q2FWG9), and PhoP (Q2FXN6) were also up-regulated, whereas two TFs (Q2FVV2, Q2G2H0), a peptide ABC (Q2G168), and the virulence factors EsxA (Q2G189) and Psm (Q2FZA4) were down-regulated. Rot, a global TF, negatively regulates the transcription of several known virulence factors, such as lipase (*geh*), hemolysins (*hla* and *hlb*), and proteases (*splA-splF*, *sspB*, and *sspC*) (McNamara et al. 2000; Said-Salim et al. 2003), and positively regulates the expression of *sarS* and other genes, including those encoding cell surface adhesins (*clfB*, *sdrC*, and *spa*). Rot and Agr have opposing effects on several genes. Another helix-turn-helix (HTH) type global TF, SarR, negatively regulates *sarA* transcription (Manna and Cheung 2001, 2006). Additionally, it negatively regulates expression of RNAII and RNAIII primary transcripts in the Agr locus. EsxA (Q2G189) plays a role as a partial virulence factor belonging to the ESAT-6 secretion system (Sundaramoorthy et al. 2008). Psm (Q2FZA4) is a phenol soluble modulin produced by the Psm-alpha gene cluster that enhances virulence and destruction of white blood cells and increases infectivity (Wang et al. 2007). Psm is promoted by phosphorylated AgrA.

Twenty-two other TCRS proteins were annotated by KEGG pathway analysis, including the histidine kinases NreB (Q2FVM6) and KapB (Q2FZV0), the alkaline phosphatase PhoA (Q2FUY6), and the TF AgrA (Q2FWM4), VraR (Q2FX09), and SrrA (Q2FY79). NreB belongs to the NreB/NreC family and is involved in the control of dissimilatory nitrate/nitrite reduction in response to low oxygen. PhoA acts in phosphate assimilation in response to phosphate limitation. AgrA is an Agr response protein (Wang and Muir 2016). VraR (Q2FX09) functions similarly to a LuxR-type HTH TF by stimulating peptidoglycan synthesis to promote cell wall formation. SrrA (Q2FY79), a global regulator of *S. aureus* virulence factors in response to environmental oxygen levels, is involved in the TCRS SrrA/SrrB system. SrrA binds to *agr*, *spa*, and *tst* promoters and represses their transcription under low oxygen conditions (Yarwood et al. 2001; Pragman et al. 2004). However, in this study SSrA was not differentially expressed between the two groups. In addition, we identified a bacitracin ABC transporter (Q2G0D8) and two acetyl-CoA

acetyltransferases (Q2G0K2 and Q2G124) in *S. aureus* 1.1861.

Agr is the main QS pathway associated with *S. aureus* virulence and consists of AgrC/A TCRS (Wang and Muir 2016). In this study, the HK AgrC was not identified. However, AgrA (Q2FWM4), a crucial regulator in the QS circuit of *S. aureus*, was identified. Two oligopeptide ABC transporters, OppA (A0A1D4HL93) and OppD (Q2FYQ7), were also found in the *S. aureus* 1.1861 proteome (Canovas et al. 2016). AIP can bind to AgrC and phosphorylate AgrA to stimulate the expression of RNAIII (Wang et al. 2014). At high cell densities, the Agr system provides positive feedback to AIP and increases the secretion of virulence factors (Pollitt et al. 2014). Therefore, we hypothesize that, in *S. aureus*, cFP is transported by membrane transporters such as OppA and OppD and binds directly to AgrA without the need for AgrC, then activates TF signal transducers and regulators at a large scale. Due to sequence divergence among the four Agr groups (Canovas et al. 2016), it is also possible that another unidentified AgrC receptor recognizes cFP in *S. aureus* 1.1861. In fact, cFP did not increase Agr system positive feed-back but instead significantly down-regulated AgrA (Q2FWM4, cFP/CK log2 fold change = − 0.5507). However, cFP did up-regulate Rot (Q9RFJ6; cFP/CK log2 fold change = 0.7715), which is a major repressor of virulence that has opposing effects on certain genes modified by Agr. SarR (Q9F0R1), which competes with AgrA to bind the P2 and P3 promoters and inhibit *agr*B, *agr*D, *agr*C, and *agr*A transcription, was also up-regulated (cFP/CK log2 fold change = 0.4325). However, EsxA (Q2G189; cFP/CK log2 fold change = − 0.6866) and the important virulence factor Psm (Q2FZA4; cFP/CK log2 fold change = − 1.1924) that is activated by AgrA, were both down-regulated. These results suggest that cFP did not activate the Agr system but seemed to play the opposite role to that of the octapeptide AIP in the Agr QS system of *S. aureus*. cFP acted similarly to a competitive inhibitor or a QS quenching agent that binds to AgrC/AgrA to inhibit phosphorylation and suppress cognate accessory gene expression due to its similar conformation to the octapeptide but not the endogenous AIP. Because four *S. aureus* subgroups can block QS via their AIPs (AIP1, AIP2, AIP3, and AIP4) (Otto et al. 2001; Tal-Gan et al. 2016), they are cross-inhibitory to the *S. aureus* Agr system. This indicates that each AgrC can only recognize its endogenous AIP and is repressed by similarly structured molecules. Li et al. (2011) demonstrated a similar phenomenon. These observations suggest that cFP may interfere with the Agr system, decrease toxin and enzyme expression, increase lipid and amino acid metabolism by promoting acetylation and phosphorylation, and reduce alcohol dehydrogenase expression.

ConclusionsA total of 1296 proteins were identified in the *S. aureus* 1.1861 proteome. KEGG pathway annotation indicated that the greatest number of proteins (77) were associated with carbon metabolism, whereas 22 proteins belonged to signal transduction, 19 proteins were ABC transporters, and 11 proteins were associated with infectious diseases. Additionally, 1038 genes were annotated by COG, including 29 signal transduction proteins, 11 intracellular trafficking, secretion and vesicular transport proteins, and 13 defense mechanism proteins. In total, 43 proteins were up-regulated and 41 proteins were down-regulated between control and treatment groups. A total of 12 proteins related to transcription and signal transduction were differentially expressed. Among the DEPs, the most significant were those which are known to be involved in amino acid metabolism, lipid metabolism, and metabolism of cofactors and vitamins. The results also showed that AgrA (Q2FWM4) exists in *S. aureus* 1.1861. Furthermore, cFP down-regulated AgrA and the virulence factors EsxA (Q2G189) and Psm (Q2FZA4) and up-regulated Rot (Q9RFJ6) and SarR (Q9F0R1), which inhibits Agr system transcription. These findings suggest that cFP can reduce Agr system expression.

Acknowledgments We thank Guangzhou Sagene Biotech Co., Ltd. for help implementing the iTRAQ proteomic experiment.

Funding Research reported in this publication was supported by the National Natural Science Foundation of China (NSFC grant numbers 31460425, 31560442, 31760466, and 31360405).

Compliance with ethical standards

Conflict of interest The authors declare that they have no conflict of interest.

Research involving human participants and/or animals None.

Informed consent None.

References

Banerjee G, Arun K (2017) Quorum-sensing network-associated gene regulation in gram-positive bacteria. Acta Microbiol Immunol Hung 64:439–453

Bassler BL (1999) How bacteria talk to each other: regulation of gene expression by quorum sensing. Curr Opin Microbiol 2:582–587

Bellezza I, Peirce MJ, Minelli A (2014) Cyclic dipeptides: from bugs to brain. Trends Mol Med 20:551–558

Bettenworth V, Steinfeld B, Duin H, Petersen K, Streit WR, Bischofs I, Becker A (2019) Phenotypic heterogeneity in bacterial quorum sensing systems. J Mol Biol. https://doi.org/10.1016/j.jmb.2019.04.036

Bina XR, Taylor DL, Vikram A, Ante VM, Bina JE (2013) *Vibrio cholerae* ToxR down regulates virulence factor production in response to cyclo (Phe-pro). MBio 4:e00366–e00313

Boles BR, Horswill AR (2008) Agr-mediated dispersal of *Staphylococcus aureus* biofilms. PLoS Pathog 4:e1000052

Brack C, Mikolasch A, Schauer F (2014) 2, 5-Diketopiperazines produced by *Bacillus pumilus* during Bacteriolysis of *Arthrobacter citreus*. Mar Biotechnol 16:385–395

Brauns SC, Milne P, Naude R, Van de Venter M (2004) Selected cyclic dipeptides inhibit cancer cell growth and induce apoptosis in HT-29 colon cancer cells. Anticancer Res 24:1713–1719

Brauns SC, Dealtry G, Milne P, Naude R, Van de Venter M (2005) Caspase −3 activation and induction of PARP cleavage by cyclic dipeptide cyclo(Phe-pro) in HT-29 cells. Anticancer Res 25:4197–4202

Canovas J, Baldry M, Bojer MS, Andersen PS, Gless BH, Grzeskowiak PK, Stegger M, Damborg P, Olsen CA, Ingmer H (2016) Cross-talk between *Staphylococcus areus* and other staphylococcal species via the agr quorum sensing system. Front Microbiol 7:1733–1745

Chai Y, Zhao M (2017) ITRAQ-based quantitative proteomic analysis of the inhibitory effects of polysaccharides from *Viscum coloratum (Kom.) Nakai* on HepG2 cells. Sci Rep 7:4596

Chen C, Ye Y, Wang R, Zhang Y, Wu C, Debnath SC, Ma Z, Wang J, Wu M (2018) *Streptomyces nigra sp. nov.* is a novel actinobacterium isolated from mangrove soil and exerts a potent antitumor activity in vitro. Front Microbiol 9:1587. https://doi.org/10.3389/fmicb.2018.01587

Daniels R, Reynaert S, Hoekstra H, Verreth C, Janssens J, Braeken K, Fauvart M, Beullens S, Heusdens C, Lambrichts I, De Vos DE, Vanderleyden J, Vermant J, Michiels J (2006) Quorum signal molecules as biosurfactants affecting swarming in *Rhizobium etli*. Proc Natl Acad Sci U S A 103:14965–14970

DeSouza L, Diehl G, Rodrigues MJ, Guo J, Romaschin AD, Colgan TJ, Siu KW (2005) Search for cancer markers from endometrial tissues using differentially labeled tags iTRAQ and cICAT with multidimensional liquid chromatography and tandem mass spectrometry. J Proteome Res 4:377–386

Duiyuan A (2017) Cyclo-pro-Phe effects on *Staphylococcus aureus* growth and energy metabolism. Res J Biotechnol 12:99–104

Eickhoff MJ, Bassler BL (2018) SnapShot: Bacterial Quorum Sensing. Cell 174:1328–1328.e1. https://doi.org/10.1016/j.cell.2018.08.003

Gillaspy AF, Worrell V, Orvis J, Roe BA, Dyer DW, Iandolo JJ (2006) The *Staphylococcus aureus* NCTC 8325 genome. In: Fischetti V (ed) Gram positive pathogens, 2nd edn. ASM Press, Washington DC, pp 381–412

Holowachuk SA, Bal'a MF, Buddington RK (2003) A kinetic microplate method for quantifying the antibacterial properties of biological fluids. J Microbiol Methods 55:441–446

Holowachuk SA, Bal'a MF, Gerard PD, Buddington RK (2004) Nonparallel secretion of antibacterial activity and protein in porcine pancreatic juice. Pancreas 28:E32–E38

Hong S, Moon BH, Yong Y, Shin SY, Lee YH, Lim Y (2008) Inhibitory effect against akt by cyclic dipeptides isolated from *Bacillus sp*. J Microbiol Biotechnol 18:682–685

Hu Z, Shi-wei S, Hui L, Aiping C, Yu-chen L, Jin Q, Ya-ling S (2019) Significantly improved production of Welan gum by *Sphingomonas sp*. WG through a novel quorum-sensing-interfering dipeptide cyclo(L-pro-L-Phe). Int J Biol Macromol 126:118–122

Huang R, Zhou X, Xu T, Yang X, Liu Y (2010) Diketopiperazines from marine organisms. Chem Biodivers 7:2809–2829

Ji G, Beavis RC, Novick RP (1995) Cell density control of staphylococcal virulence mediated by an octapeptide pheromone. Proc Natl Acad Sci U S A 92:12055–12059

Jiang Q, Chen J, Yang C, Yin Y, Yao K (2019) Quorum sensing: a prospective therapeutic target for bacterial diseases. Biomed Res Int 2019:2015978. https://doi.org/10.1155/2019/2015978

Kanehisa M, Araki M, Goto S, Hattori M, Hirakawa M, Itoh M, Katayama T, Kawashima S, Okuda S, Tokimatsu T, Yamanishi Y (2008) KEGG for linking genomes to life and the environment. Nucleic Acids Res 36:D480–D484

Kavanaugh JS, Horswill AR (2016) Impact of environmental cues on staphylococcal quorum sensing and biofilm development. J Biol Chem 291:12556–12564

Kim IH, Son JS, Wen Y, Jeonq SM, Min GY, Park NY, Lee KW, Cho YJ, Chun J, Kim KS (2013) Transcriptomic analysis of genes modulated by cyclo(L-phenylalanine-L-proline) in *Vibrio vulnificus*. J Microbiol Biotechnol 23:1791–1801

Kim K, Kim NJ, Kim SY, Kim IH, Kim KS, Lee GR (2015) Cyclo(Phe-pro) produced by the human pathogen *Vibrio vulnificus* inhibits host innate immune responses through the NF-κB pathway. Infect Immun 83:1150–1161

Kumari A, Pasini P, Deo SK, Flomenhoft D, Shashidhar S, Daunert S (2006) Biosensing systems for the detection of bacterial quorum signaling molecules. Anal Chem 78:7603–7609

Kwak MK, Liu R, Kang SO (2018) Antimicrobial activity of cyclic dipeptides produced by *Lactobacillus plantarum LBP-K10* against multidrug-resistant bacteria, pathogenic fungi, and influenza a virus. Food Control 85:223–234

Lee W, Lee SH, Kim M, Moon JS, Kim GW, Jung HG, Kim IH, Oh JE, Jung HE, Lee HK, Ku KB, Ahn DG, Kim SJ, Kim KS, Oh JW (2018) *Vibrio vulnificus* quorum-sensing molecule cyclo (Phe-pro) inhibits RIG-I-mediated antiviral innate immunity. Nat Commun 9:1606. https://doi.org/10.1038/s41467-018-04075-1

Li J, Wang W, Xu SX, Magarvey NA, McCormick JK (2011) *Lactobacillus reuteri*-produced cyclic dipeptides quench agr-mediated expression of toxic shock syndrome toxin-1 in staphylococci. Proc Natl Acad Sci U S A 108:3360–3365

Manna AC, Cheung AL (2001) Characterization of sarR, a modulator of Sar expression in *Staphylococcus aureus*. Infect Immun 69:885–896

Manna AC, Cheung AL (2006) Transcriptional regulation of the agr locus and the identification of DNA binding residues of the global regulatory protein SarR in *Staphylococcus aureus*. Mol Microbiol 60:1289–1301

McNamara PJ, Milligan-Monroe KC, Khalili S, Proctor RA (2000) Identification, cloning, and initial characterization of rot, a locus encoding a regulator of virulence factor expression in *Staphylococcus aureus*. J Bacteriol 182:3197–3203

Mishra AK, Choi J, Choi SJ, Baek KH (2017) Cyclodipeptides: an overview of their biosynthesis and biological activity. Molecules 22. DOI: https://doi.org/10.3390/molecules22101796

Otto M, Echner H, Voelter W, Gotz F (2001) Pheromone cross-inhibition between *Staphylococcus aureus* and *Staphylococcus epidermidis*. Infect Immun 69:1957–1960. https://doi.org/10.1128/IAI.69.3.1957-1960.200

Pan J, Ren D (2009) Quorum sensing inhibitors: a patent overview. Expert Opin Ther Pat 19:1581–1601

Park DK, Lee KE, Baek CH, Kim IH, Kwon IH, Lee WK, Lee KH, Kim BS, Choi SH, Kim KS (2006) Cyclo(Phe-pro) modulates the expression of ompU in *Vibrio spp*. J Bacteriol 188:2214–2221

Peterson S, Cline RT, Tettelin H, Sharov V, Morrison DA (2000) Gene expression analysis of the *Streptococcus pneumoniae* competence regulons by use of DNA micro-arrays. J Bacteriol 182:6192–6202

Pollitt EJ, West SA, Crusz SA, Burton-Chellew MN, Diggle SP (2014) Cooperation, quorum sensing, and evolution of virulence in *Staphylococcus aureus*. Infect Immun 82:1045–1051

Pragman AA, Yarwood JM, Tripp TJ, Schlievert PM (2004) Characterization of virulence factor regulation by SrrAB, a two-component system in *Staphylococcus aureus*. J Bacteriol 186(8):2430–2438

Prasad C (1995) Bioactive cyclic dipeptides. Peptides 16:151–164

Rhee KH (2004) Cyclic dipeptides exhibit synergistic, broad spectrum antimicrobial effects and have anti-mutagenic properties. Int J Antimicrob Agents 24:423–427

Ross PL, Huang YN, Marchese JN, Williamson B, Parker K, Hattan S, Khainovski N, Pillai S, Dey S, Daniels S, Purkayastha S, Juhasz P, Martin S, Bartlet-Jones M, He F, Jacobson A, Pappin DJ (2004) Multiplexed protein quantitation in *Saccharomyces cerevisiae* using amine reactive isobaric tagging reagents. Mol Cell Proteomics 3:1154–1169

Rutherford ST, Bassler BL (2012) Bacterial quorum sensing: its role in virulence and possibilities for its control. Cold Spring Harb Perspect Med 2:a012427

Said-Salim B, Dunman PM, McAleese FM, Macapagal D, Murphy E, McNamara PJ, Arvidson S, Foster TJ, Projan SJ, Kreiswirth BN (2003) Global regulation of *Staphylococcus aureus* genes by rot. J Bacteriol 185:610–619

Sundaramoorthy R, Fyfe PK, Hunter WN (2008) Structure of *Staphylococcus aureus* EsxA suggests a contribution to virulence by action as a transport chaperone and/or adaptor protein. J Mol Biol 383:603–614

Tal-Gan Y, Ivancic M, Cornilescu G, Blackwell HE (2016) Characterization of structural elements in native autoinducing peptides and non-native analogues that permit the differential modulation of AgrC-type quorum sensing receptors in *Staphylococcus aureus*. Org Biomol Chem 14:113–121. https://doi.org/10.1039/c5ob01735a

Tang K, Zhang XH (2014) Quorum quenching agents: resources for antivirulence therapy. Mar Drugs 12:3245–3282

Thoendel M, Kavanaugh JS, Flack CE, Horswill AR (2011) Peptide signaling in the staphylococci. Chem Rev 111:117–151

Vuong C, Saenz HL, Gotz F, Otto M (2000) Impact of the agr quorum-sensing system on adherence to polystyrene in *Staphylococcus aureus*. J Infect Dis 182:1688–1693

Wang B, Muir TW (2016) Regulation of virulence in *Staphylococcus aureus*: molecular mechanisms and remaining puzzles. Cell Chem Biol 23(2):214–224

Wang R, Braughton KR, Kretschmer D, Bach TH, Queck SY, Li M, Kennedy AD, Dorward DW, Klebanoff SJ, Peschel A, DeLeo FR, Otto M (2007) Identification of novel cytolytic peptides as key virulence determinants for community-associated MRSA. Nat Med 13:1510–1514

Wang B, Zhao A, Novick RP, Muir TW (2014) Activation and inhibition of the receptor histidine kinase AgrC occurs through opposite helical transduction motions. Mol Cell 53:929–940

Wei Y, Perez LJ, Ng WL, Semmelhack MF, Bassler BL (2011) Mechanism of *Vibrio cholerae* autoinducer-1 biosynthesis. ACS Chem Biol 6:356–365

Wiese S, Reidegeld KA, Meyer HE, Warscheid B (2007) Protein labeling by iTRAQ: a new tool for quantitative mass spectrometry in proteome research. Proteomics 7:340–350

Xiao YY, Kuang JF, Qi XN, Ye YJ, Wu ZX, Chen JY, Lu WJ (2017) A comprehensive investigation of starch degradation process and identification of a transcriptional activator MabHLH6 during banana fruit ripening. Plant Biotechnol J 16:151–164

Yarwood JM, McCormick JK, Schlievert PM (2001) Identification of a novel two-component regulatory system that acts in global regulation of virulence factors of *Staphylococcus aureus*. J Bacteriol 183(4):1113–1123

Yarwood JM, Bartels DJ, Volper EM, Greenberg EP (2004) Quorum sensing in *Staphylococcus aureus* biofilms. J Bacteriol 186:1838–1850

Zhang Q, Huang S, Luo H, Zhao X, Wu G, Wu D (2017) Eight-plex iTRAQ labeling and quantitative proteomic analysis for human bladder cancer. Am J Cancer Res 7:935–945

Zhao J, Li X, Hou X, Quan C, Chen M (2019) Widespread Existence of Quorum Sensing Inhibitors in Marine Bacteria: Potential Drugs to Combat Pathogens with Novel Strategies. Mar Drugs 17(5). DOI: https://doi.org/10.3390/md17050275